

# Protein kinase A-mediated phosphorylation of naked cuticle homolog 2 stimulates cell-surface delivery of transforming growth factor- $\alpha$ for epidermal growth factor receptor transactivation

Zheng Cao<sup>1,2</sup> | Bhuminder Singh<sup>1,2,3</sup>  | Cunxi Li<sup>4,5</sup> | Nicholas O. Markham<sup>1,2</sup>  |  
Léolène J. Carrington<sup>1</sup>  | Jeffrey L. Franklin<sup>1,2,3,6</sup>  | Ramona Graves-Deal<sup>1,2</sup> |  
Eileen J. Kennedy<sup>7</sup>  | James R. Goldenring<sup>2,3,6,8</sup>  | Robert J. Coffey<sup>1,2,3,6</sup> 

<sup>1</sup>Department of Medicine, Vanderbilt University Medical Center, Nashville, Tennessee

<sup>2</sup>Epithelial Biology Center, Vanderbilt University School of Medicine, Nashville, Tennessee

<sup>3</sup>Department of Cell and Developmental Biology, Vanderbilt University, Nashville, Tennessee

<sup>4</sup>Jiaen Genetics Laboratory, Beijing Jiaen Hospital, Beijing, China

<sup>5</sup>Genetics Center, Shenzhen IVF Gynecology Hospital, Shenzhen, China

<sup>6</sup>Department of Medicine, Veterans Affairs Medical Center, Nashville, Tennessee

<sup>7</sup>Department of Pharmaceutical and Biomedical Sciences, College of Pharmacy, University of Georgia, Athens, Georgia

<sup>8</sup>Department of Surgery, Vanderbilt University School of Medicine, Nashville, Tennessee

## Correspondence

Robert J. Coffey, Epithelial Biology Center, 10415 MRB IV, Vanderbilt University Medical Center, Nashville, TN 37232-0441.  
Email: robert.coffey@vumc.org

## Funding information

National Cancer Institute, Grant/Award Numbers: P30 CA068485, P50 95103, R03 CA188439, R35 CA197570; National Institute of Diabetes and Digestive and Kidney Diseases, Grant/Award Numbers: P30 DK058404, R01 DK48370, R01 DK70856

## Peer Review

The peer review history for this article is available at <https://publons.com/publon/10.1111/tra.12642>

## Abstract

The classic mode of G protein-coupled receptor (GPCR)-mediated transactivation of the receptor tyrosine kinase epidermal growth factor receptor (EGFR) transactivation occurs via matrix metalloprotease (MMP)-mediated cleavage of plasma membrane-anchored EGFR ligands. Herein, we show that the G $\alpha$ s-activating GPCR ligands vasoactive intestinal peptide (VIP) and prostaglandin E<sub>2</sub> (PGE<sub>2</sub>) transactivate EGFR through increased cell-surface delivery of the EGFR ligand transforming growth factor- $\alpha$  (TGF $\alpha$ ) in polarizing madin-darby canine kidney (MDCK) and Caco-2 cells. This is achieved by PKA-mediated phosphorylation of naked cuticle homolog 2 (NKD2), previously shown to bind TGF $\alpha$  and direct delivery of TGF $\alpha$ -containing vesicles to the basolateral surface of polarized epithelial cells. VIP and PGE<sub>2</sub> rapidly activate protein kinase A (PKA) that then phosphorylates NKD2 at Ser-223, a process that is facilitated by the molecular scaffold A-kinase anchoring protein 12 (AKAP12). This phosphorylation stabilized NKD2, ensuring efficient cell-surface delivery of TGF $\alpha$  and increased EGFR activation. Thus, GPCR-triggered, PKA/AKAP12/NKD2-regulated targeting of TGF $\alpha$  to the cell surface represents a new mode of EGFR transactivation that occurs proximal to ligand cleavage by MMPs.

## KEYWORDS

A-kinase anchoring protein 12 (AKAP12), EGFR transactivation, epidermal growth factor receptor (EGFR), G protein-coupled receptor (GPCR), naked cuticle homolog 2 (NKD2), protein kinase A (PKA), transforming growth factor- $\alpha$  (TGF $\alpha$ )

Zheng Cao and Bhuminder Singh should be considered joint first author.

This is an open access article under the terms of the Creative Commons Attribution-NonCommercial License, which permits use, distribution and reproduction in any medium, provided the original work is properly cited and is not used for commercial purposes.

© 2019 The Authors. Traffic published by John Wiley & Sons Ltd.

## 1 | INTRODUCTION

G-protein-coupled receptors (GPCRs) and receptor tyrosine kinases (RTKs) comprise a large proportion of cell-surface receptors that sense and respond to extracellular stimuli employing distinct signal transducers to execute downstream signaling.<sup>1,2</sup> A point of convergence between GPCRs and RTKs at the cell surface is the phenomenon of GPCR-induced RTK transactivation.<sup>3,4</sup> The first identified and best-studied example is EGFR transactivation.<sup>5</sup> Most often, this is achieved by activation of cell-surface matrix metalloproteases (MMPs), which cleave the ectodomain of membrane-anchored EGFR ligands to release soluble ligands that then bind and activate EGFRs.<sup>6</sup>

A number of GPCR signal transducers have been implicated in EGFR transactivation via MMP activation, including the  $\alpha$ ,  $\beta$  and  $\gamma$  subunits of heterotrimeric G proteins.<sup>3</sup> For example, activated  $G_{\alpha s}$  associates with and activates adenylyl cyclase, which catalyzes the release of the secondary messenger cyclic adenosine monophosphate (cAMP).<sup>7</sup> cAMP subsequently activates other proteins including protein kinase A (PKA), which has been shown to stimulate MMP activity.<sup>8</sup> Localized PKA activity in the cell is achieved by more than 50 human PKA-interacting scaffolding proteins, designated A-kinase anchoring proteins (AKAPs), that directly bind PKA and target it to specific subcellular locations.<sup>9</sup> On the other hand,  $G_{\alpha q}$  activates phospholipase C, which cleaves phosphatidylinositol 4,5-bisphosphate (PIP<sub>2</sub>) into inositol 1,4,5-trisphosphate (IP<sub>3</sub>) and diacylglycerol (DAG); DAG in turn activates protein kinase C (PKC), which also has been shown to induce MMP-dependent shedding of EGFR ligands.<sup>10</sup>

TGF $\alpha$  is one of seven mammalian EGFR ligands that are produced as type 1 transmembrane proteins.<sup>11–13</sup> In polarized epithelial cells, the TGF $\alpha$  precursor is delivered preferentially to the basolateral cell surface where it undergoes ectodomain cleavage by a selective MMP, a disintegrin and a metalloprotease 17 (ADAM17). This cleavage releases soluble TGF $\alpha$ , which is then rapidly captured by basolateral EGFRs.<sup>14</sup> We previously showed that the protein naked cuticle homolog 2 (NKD2) acts as basolateral sorting adaptor for TGF $\alpha$ .<sup>15</sup> NKD2 coats TGF $\alpha$ -containing exocytic vesicles by interacting directly with the TGF $\alpha$  cytoplasmic domain. These vesicles are then directed to the basolateral surface of polarized epithelial cells where they dock and fuse in a NKD2 myristoylation-dependent manner.<sup>15,16</sup> NKD2 is a short-lived protein with a half-life of approximately 2 hours and is targeted for degradation by the RING-finger E3 ubiquitin-protein ligase (RNF25).<sup>17</sup>

Herein, we have discovered that NKD2 is phosphorylated at serine 223 (S223) after stimulation with GPCR agonists, VIP and PGE<sub>2</sub>, via activation of PKA. NKD2 phosphorylation by PKA is dependent on the molecular scaffold AKAP12. This phosphorylation stabilizes NKD2, promoting efficient cell-surface delivery of TGF $\alpha$  and results in increased EGFR activation. Thus, these studies identify a new mode of GPCR-triggered EGFR transactivation that occurs proximal to MMP cleavage of plasma membrane-anchored ligands.

## 2 | RESULTS

### 2.1 | PKA phosphorylates NKD2 at S223

Based on our previous results showing that myristoylation and ubiquitylation of NKD2 affect its function, we set out to determine whether NKD2 was also phosphorylated and the possible functional consequence of such phosphorylation.<sup>13,15,17</sup> To that end, we labeled MDCK cells stably expressing NKD2-enhanced green fluorescent protein (EGFP) with <sup>32</sup>P-ATP and found that NKD2 was phosphorylated under steady state conditions (Figure 1A). To identify potential phosphorylation sites on NKD2, we conducted an *in silico* protein phosphorylation prediction analysis (NetPhos).<sup>18</sup> Six potential PKA phosphorylation sites (S18, S216, S223, S286, S299 and S337) and 16 potential PKC phosphorylation sites were identified (Table S1). To activate PKA or PKC, NKD2-EGFP-overexpressing MDCK cells were stimulated with forskolin (FSK, 1  $\mu$ M) or 12-O-tetradecanoylphorbol-13-acetate (TPA, 100 nM), respectively, for various times. Cells were then lysed and subjected to NKD2 immunoprecipitation (IP) and subsequent immunoblotting with antibodies that recognize a consensus phosphorylated PKA (pPKA) substrate motif [RXXp(S/T)]<sup>19,20</sup>, or a consensus phosphorylated PKC (pPKC) substrate motif [(R/K)Xp(S) (R/K)].<sup>21</sup> As early as 1 minute after addition of FSK, there was a marked increase in pPKA substrate motif in NKD2-EGFP IPs, and the signal was sustained over the 30-minute time course (Figure 1B, upper panel). In marked contrast, addition of TPA failed to elicit a signal in NKD2 IPs using the pPKC substrate motif antibody (Figure 1B, bottom panel). AKAP12-EGFP was transiently expressed in the presence or absence of TPA as a positive control for the pPKC substrate motif antibody; TPA treatment showed the expected increase in phosphorylation of PKC substrates (Figure S1). NKD1 is an ortholog of NKD2 with 44% overall homology. However, NKD1 does not contain a PKA consensus site, and FSK did not induce NKD1 phosphorylation in NKD1-EGFP-overexpressing MDCK cells as determined using the pPKA substrate motif antibody (Figure 1C). Thus PKA, but not PKC, selectively phosphorylates NKD2.

To determine the specific residue(s) phosphorylated by PKA, all six potential PKA phosphorylation sites in NKD2-EGFP were mutated to alanine individually and transiently expressed in human embryonic kidney 293 (HEK293) cells; these cells were then stimulated with FSK. Only the (S223A)NKD2 mutant failed to show a signal with the pPKA substrate motif antibody in NKD2-EGFP IP, indicating selective phosphorylation at S223 (Figure 1D). Of note, NKD2 S223 lies within a consensus pPKA substrate motif (RRPST). We next generated a phosphorylation-specific polyclonal antibody by immunizing rabbits against the NKD2 phospho-peptide HVRRPpSTDpQPC containing S223 (see Section 4). The pS223-NKD2 antibody detected a single band following FSK stimulation, and this increase was attenuated by pretreatment with the PKA inhibitor H89 (Figure 1E, top panel). Results with the pS223-NKD2 antibody mirrored those using the pPKA substrate motif antibody (compare Figure 1E top and middle panels). No signal was detected with pS223-NKD2 or pPKA substrate motif

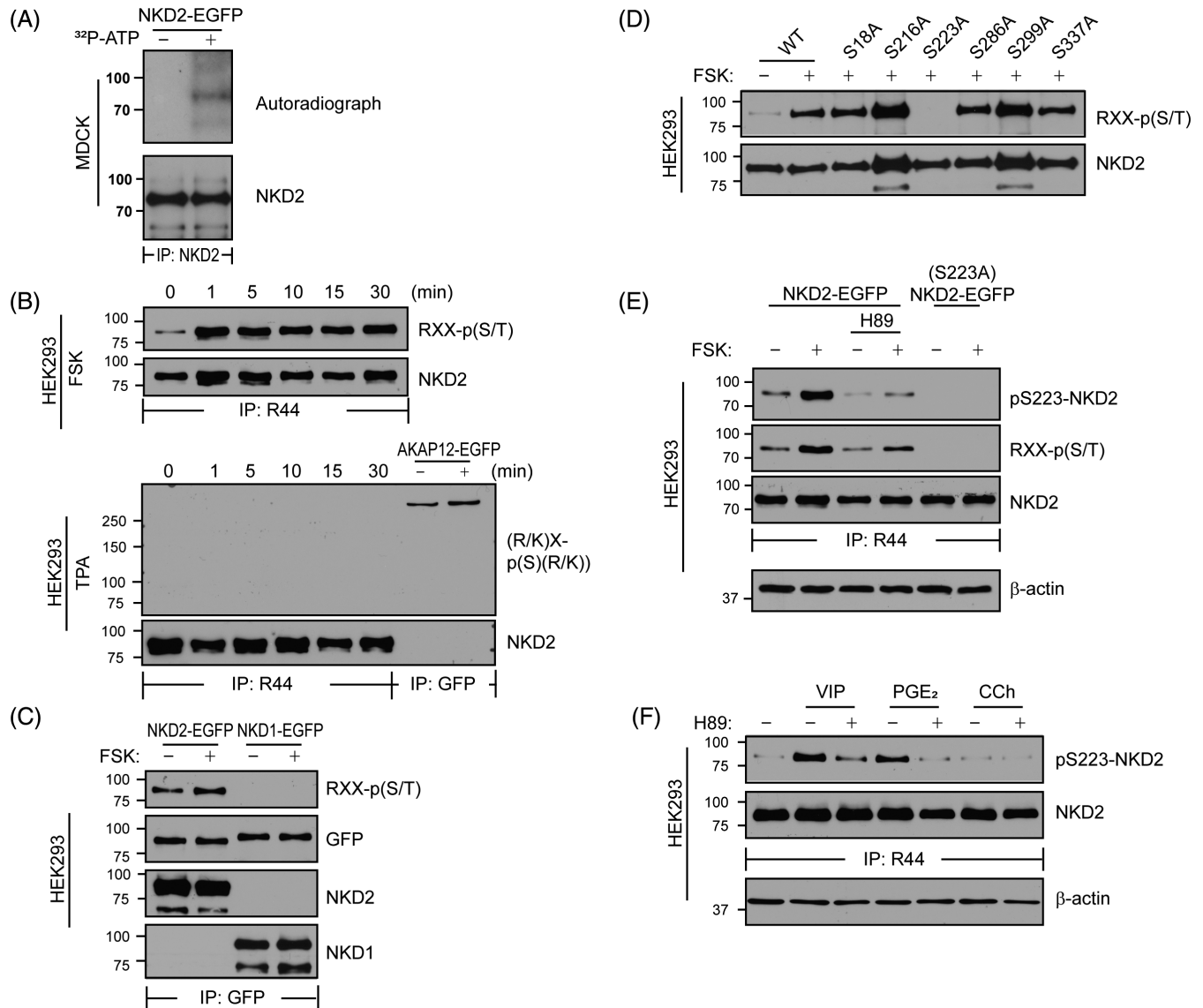


**FIGURE 1** PKA phosphorylates NKD2 at serine 223. A, MDCK cells stably expressing NKD2-EGFP were labeled with  $^{32}\text{P}$ -ATP at  $37^\circ\text{C}$  for 2 hours, at which time cells were lysed and subjected to NKD2 immunoprecipitation (IP). The top panel (autoradiograph) shows incorporation of radiolabel in the NKD2 IP. The bottom panel shows NKD2 immunoblotting of the IPs as loading control from a parallel western blot. B, HEK293 cells stably expressing NKD2-EGFP were incubated with  $1\ \mu\text{M}$  forskolin (FSK) (top panel) or  $100\ \text{nM}$  TPA (lower panel) for the indicated times. Cell lysates were subjected to NKD2 IP with the R44 antibody against NKD2 and then immunoblotted with pPKA or pPKC substrate motif antibodies, respectively. Membranes were later reprobed with NKD2 to confirm equal loading. As a positive control, AKAP12-EGFP was expressed in the presence or absence of TPA. C, HEK293 cells transiently expressing NKD2-EGFP or NKD1-EGFP were incubated with  $1\ \mu\text{M}$  FSK for 5 minutes as indicated. Cell lysates were harvested and subjected to GFP IP, resolved on SDS-PAGE, and probed with GFP, NKD1, NKD2 and pPKA substrate motif antibodies. D, Six serine residues predicted to be PKA phosphorylation sites within NKD2 were mutated individually to alanine (S > A). HEK293 cells transiently expressing EGFP-tagged wild-type (WT) NKD2 and indicated mutants were stimulated with  $1\ \mu\text{M}$  FSK for 5 minutes. Cell lysates were harvested and subjected to NKD2 IP, resolved on SDS-PAGE and probed with antibodies against pPKA substrate motif antibody and NKD2. E, HEK293 cells transiently expressing NKD2-EGFP and (S223A)NKD2-EGFP were pretreated with the PKA inhibitor H89 ( $30\ \mu\text{M}$ , 1 hour) and subsequently incubated with  $1\ \mu\text{M}$  FSK for 5 minutes as indicated. Cell lysates were subjected to IP and immunoblotted using the indicated antibodies. F, HEK293 cells transiently expressing NKD2-EGFP were pretreated with H89 ( $30\ \mu\text{M}$ , 1 hour) as indicated and then stimulated with VIP ( $100\ \text{nM}$ ),  $\text{PGE}_2$  ( $100\ \text{ng/mL}$ ) or carbachol (CCh,  $100\ \mu\text{M}$ ) for 5 minutes. Cell lysates were subjected to NKD2 IP and immunoblotted using the indicated antibodies. Corresponding total lysates were probed with  $\beta$ -actin antibody as a loading control for (E and F)

antibodies in HEK293 cells transiently expressing (S223A) NKD2-EGFP (Figure 1E). Together, these results show that the RRPST sequence of NKD2 is a specific PKA recognition motif (Figure 1E, middle panel).

After showing NKD2 S223 phosphorylation by FSK stimulation, we next tested if physiological stimuli like GPCR agonists (e.g., VIP,  $\text{PGE}_2$  and carbachol) may induce NKD2 phosphorylation. All three ligands have previously been shown to induce EGFR

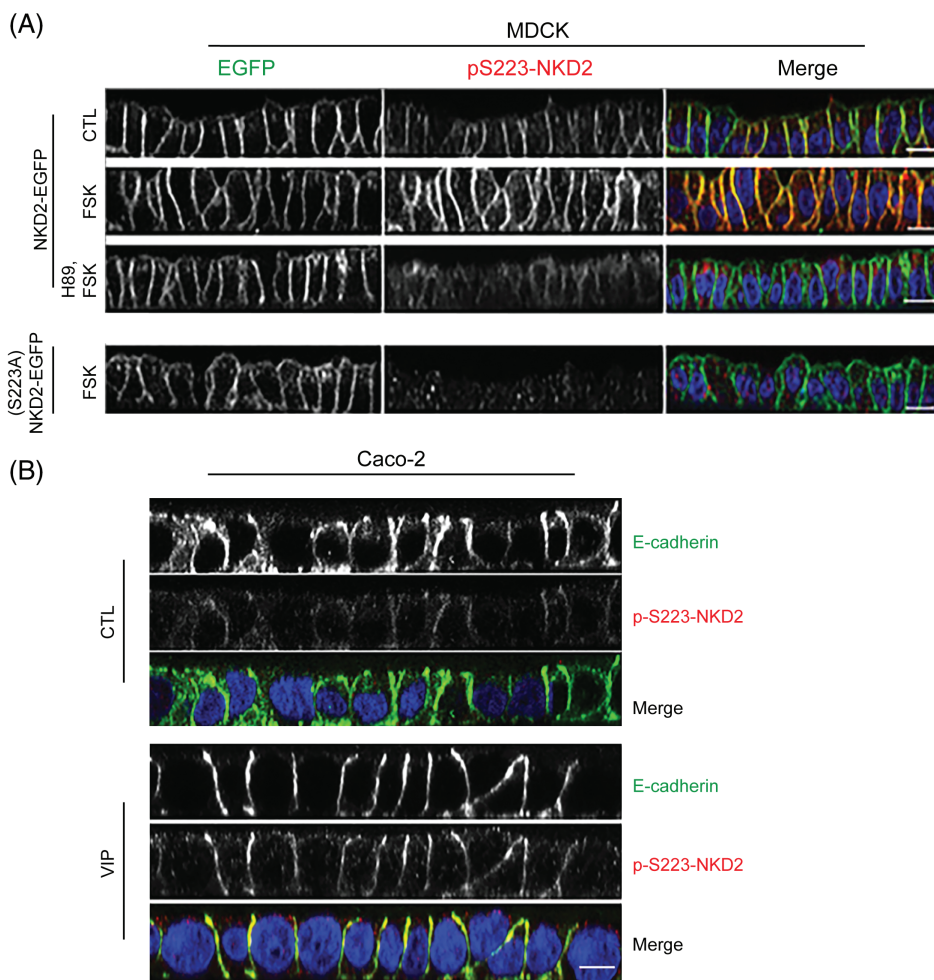


**FIGURE 2** FSK and VIP stimulate NKD2 S223 phosphorylation in polarized MDCK and Caco-2 cells, respectively. A, MDCK cells stably expressing NKD2-EGFP or (S223A)NKD2-EGFP were grown on Transwell filters for 5 days. Cells were then either left untreated (CTL) or pretreated with H89 (30  $\mu$ M, 1 hour) and/or stimulated with FSK (1  $\mu$ M, 5 minutes) as indicated. Filters were paraformaldehyde-fixed and immunostained for pS223-NKD2 (red); NKD2-EGFP fluorescence is shown in green. Confocal projections in the xz plane are shown. Scale bars: 10  $\mu$ m. B, Parental Caco-2 cells were grown on Transwell filters for 5 days. VIP (100 nM) was added to the basolateral compartment for 5 minutes (lower panel). Top panel shows untreated control (CTL). Filters were then paraformaldehyde-fixed and stained for E-cadherin (green), pS223-NKD2 (red) and nuclei (DAPI, blue). Confocal projections in the xz plane are shown. Scale bars: 10  $\mu$ m

transactivation.<sup>8,22,23</sup> VIP and PGE<sub>2</sub> elicit G $\alpha$ s downstream signaling, while carbachol activates pathways mediated by G $\alpha$ q, which in turn activate PKA and PKC, respectively. Both VIP and PGE<sub>2</sub> induced rapid NKD2 phosphorylation, which was attenuated by the PKA inhibitor H89, while carbachol failed to induce NKD2 phosphorylation as measured by pS223-NKD2 antibody, indicating that NKD2 phosphorylation is specifically induced by G $\alpha$ s-associated GPCR activation (Figure 1F).

We next used the pS223-NKD2 antibody to determine the subcellular location of phosphorylated NKD2 in fully polarized epithelial cells cultured on Transwell filters. In polarized MDCK cells stably expressing NKD2-EGFP, pS223-NKD2 antibody predominantly decorated the lateral membrane at steady state (Figure 2A). The intensity of the fluorescence increased following addition of FSK and appeared to extend further up the lateral membrane; pretreatment with H89 dramatically diminished the FSK-induced pS223-NKD2 signal. As expected, no signal was detected with this antibody after addition of FSK to polarized MDCK cells stably expressing (S223A)NKD2-EGFP (Figure 2A, bottom panel). To assess whether endogenous NKD2 was phosphorylated by GPCR agonist stimulation, we added VIP to Caco-2 cells, a human colorectal cancer cell line that expresses NKD2 endogenously and polarizes on Transwell filters.<sup>24</sup> Addition of VIP (100 nM) to the basolateral compartment markedly increased

pS223-NKD2 signal at the lateral membrane within 5 minutes (Figure 2B). In another colorectal cancer cell line, HCA-7, that also polarizes on Transwell filters and expresses NKD2 endogenously, we observed a similar increase in pS223-NKD2 staining after VIP addition (Figure S2).<sup>25</sup> Thus, activation of PKA by the GPCR ligand VIP increases phosphorylation of endogenous NKD2 at the lateral membrane.

## 2.2 | NKD2 S223A mutant exhibits a shorter half-life and results in reduced TGF $\alpha$ delivery to the cell surface

To assess the functional consequence of NKD2 S223 phosphorylation, we first examined its half-life in MDCK cells stably expressing either NKD2-EGFP or (S223A)NKD2-EGFP. Cycloheximide (CHX, 20  $\mu$ g/mL) was added to block protein synthesis, and cell lysates were prepared and immunoblotted for NKD2 and  $\alpha$ -tubulin (as a loading control) at the indicated time points (Figure 3A). Over the 8-hour time course, the NKD2 signal persisted longer in cells expressing NKD2-EGFP than (S223A)NKD2-EGFP. These results are quantified on the right in Figure 3B, where half-lives of NKD2-EGFP and (S223A)NKD2-EGFP were determined to be around 2 and 1 hour, respectively.

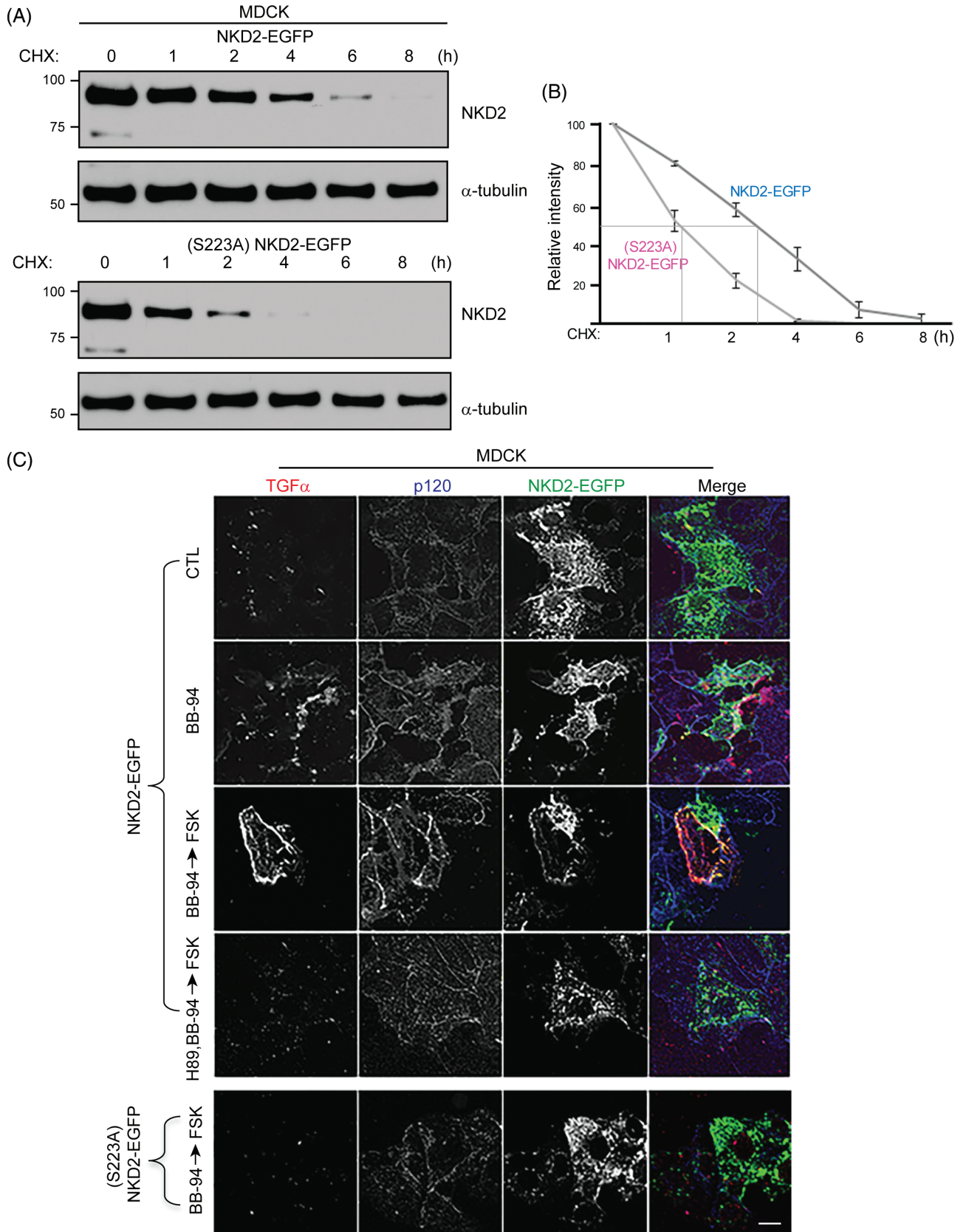


FIGURE 3 Legend on next page.

To extend this functional analysis, we transiently transfected TGF $\alpha$  into NKD2-overexpressing MDCK cells. We assessed the relative amounts of TGF $\alpha$  at the cell surface by examining TGF $\alpha$  immunoreactivity in nonpermeabilized cells after various manipulations as indicated (Figure 3C). The broad spectrum MMP inhibitor Batimastat (BB-94) was used to block cell-surface cleavage of TGF $\alpha$ . In wild-type NKD2-expressing cells, exposure to BB-94 for 1 hour led to a modest increase in cell-surface TGF $\alpha$  immunofluorescence (Figure 3C). If FSK was added to BB-94-treated cells for 5 minutes prior to TGF $\alpha$  staining, there was a marked increase in TGF $\alpha$  immunoreactivity. However, if H89 was added at the same time as BB-94, TGF $\alpha$  was not detected at the cell surface. In marked contrast to what was observed with wild-type NKD2-expressing cells, TGF $\alpha$  was not detected at the cell surface when FSK was added to BB-94-treated (S223A) NKD2-EGFP-expressing cells. Thus, (S223A)NKD2 mutant is less stable than wild-type NKD2, and cell-surface delivery of TGF $\alpha$  is impaired in cells that express a form of NKD2 that cannot be phosphorylated by PKA.

### 2.3 | EGFR transactivation by VIP is dependent on NKD2-mediated TGF $\alpha$ delivery

To evaluate how PKA phosphorylation of NKD2 might impact EGFR activity, we took two experimental approaches. In the first approach, we added conditioned medium from MDCK cells transiently expressing TGF $\alpha$  and either wild-type NKD2, (S223A)NKD2, or (G2A)NKD2 to recipient serum-starved A431 cells. The (G2A)NKD2 mutant cannot be myristoylated, and we have previously shown that this mutation prevents membrane fusion of TGF $\alpha$ -containing NKD2 vesicles.<sup>15,16</sup> Parenthetically, A431 cells express large amounts of EGFR and are often used to study the effect of EGF-like ligands.<sup>26</sup> Five minutes after addition of conditioned medium, EGFR activity was monitored in recipient cells by immunoprecipitating EGFR from whole-cell lysates and then immunoblotting with pY1173-EGFR antibody. As expected, no signal was detected with conditioned medium from parental MDCK cells (Figure 4A, lane 1), and only modest EGFR activation was observed in cells expressing TGF $\alpha$  alone (Figure 4A, last lane). The strongest signal in A431 lysates was found after addition of conditioned medium from MDCK cells expressing both wild-type NKD2 and TGF $\alpha$ . Notably, EGFR activity in A431 cells was markedly reduced after addition of conditioned medium from MDCK cells expressing (S223A)NKD2 (lane 5) and (G2A)NKD2 (lane 6) with TGF $\alpha$ ;

this signal was equivalent to cells expressing TGF $\alpha$  alone (compare lanes 5 and 6 with lane 8, Figure 4A). As additional controls, neutralizing antibodies to TGF $\alpha$  or EGFR were added to MDCK cultures 1 hour prior to harvesting of conditioned medium for addition to A431 cells. The ability of these neutralizing antibodies to block EGFR activity supports that the conditioned medium effects were attributable to TGF $\alpha$  signaling via EGFR (Figure 4A). Taken together, these results show that NKD2 regulates the release of soluble, biologically active TGF $\alpha$ .

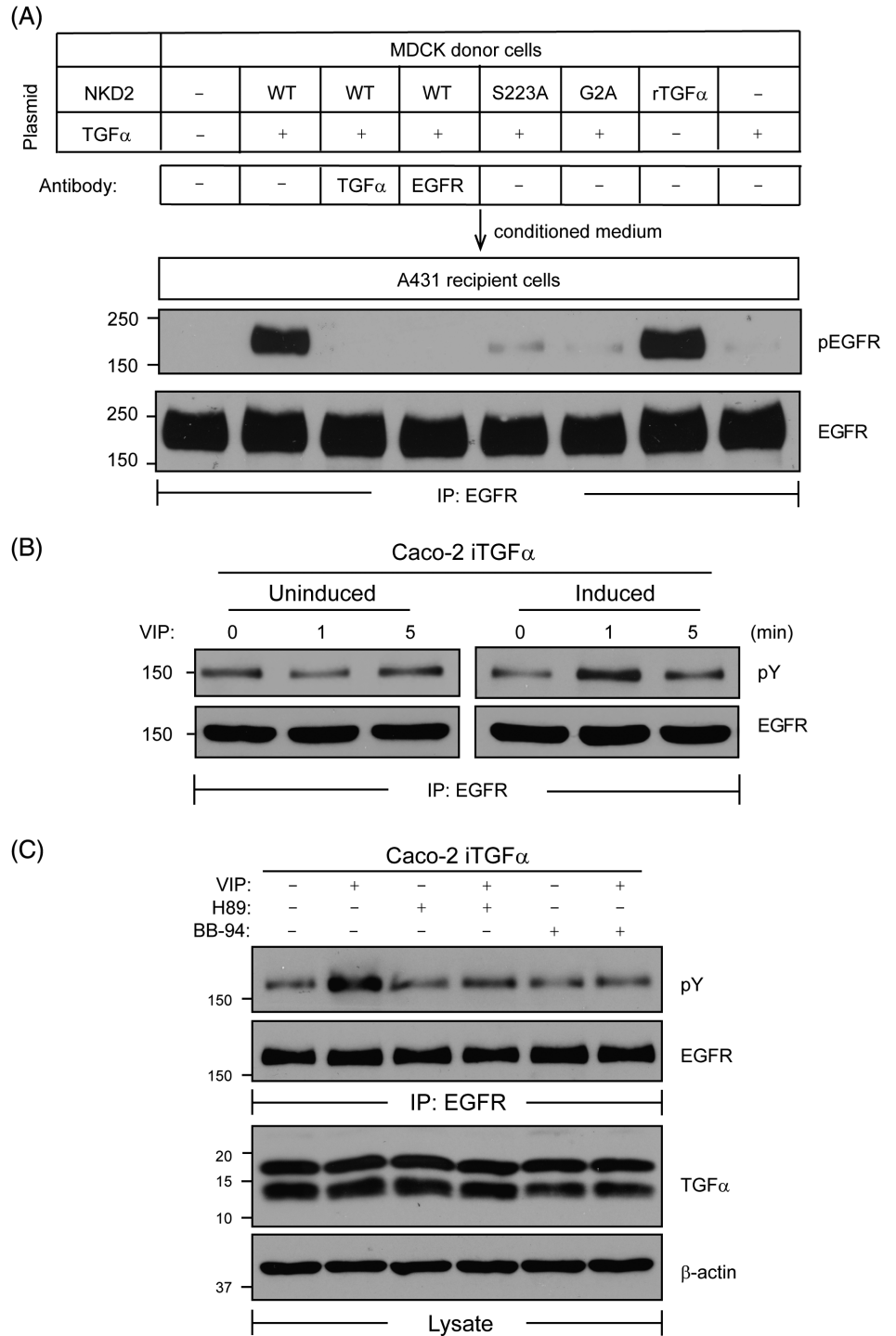
In the second approach, we added the GPCR ligand VIP to Caco-2 cells cultured on plastic to directly implicate ligand delivery in GPCR-mediated EGFR transactivation. Parental Caco-2 cells do not express TGF $\alpha$ , so we engineered these cells to stably express a doxycycline-inducible TGF $\alpha$  construct (Caco-2 iTGF $\alpha$ ). In the uninduced state, addition of VIP to Caco-2 iTGF $\alpha$  cells had no effect on EGFR activity (Figure 4B, left panel). However, in the TGF $\alpha$ -induced state, there was a dramatic increase in EGFR activity 1 minute after VIP addition (Figure 4B, right panel). In these experiments, EGFR activity was monitored by immunoblotting EGFR IPs with phospho-tyrosine (pY) antibody. In Figure 4C, we show that VIP-induced EGFR activity was markedly reduced by blocking PKA activity with H89 and blocking metalloprotease activity with BB-94 in Caco-2 iTGF $\alpha$  cells in the induced state. In fact, H89 was at least as effective as BB-94 (compare lanes 4 and 6) in blocking EGFR activity. In a similar experiment, PGE<sub>2</sub> was also able to induce EGFR phosphorylation in a PKA- and TGF $\alpha$ -dependent manner in Caco-2 iTGF $\alpha$  cells (Figure S3). Thus, under these experimental conditions, GPCR transactivation of EGFR is due to increased cell-surface delivery of TGF $\alpha$ .

### 2.4 | AKAP12 interacts with NKD2 and facilitates its phosphorylation by PKA

Localized intracellular PKA activity is achieved by PKA-interacting scaffolding proteins called AKAPs that assemble and compartmentalize multiprotein PKA signaling complexes.<sup>27,28</sup> AKAP12 was a logical candidate to examine because it was the only AKAP detected in a comprehensive proteomic analysis of NKD2-associated vesicles.<sup>29</sup> Interaction of AKAP12 and PKA has been reported previously.<sup>30–32</sup> In Figure 5A, we show that NKD2 and AKAP12 interact by reciprocal co-IP in HEK293 cells transiently expressing untagged NKD2 and AKAP12-EGFP. We also show that the two proteins colocalize in cytoplasmic puncta and at the plasma membrane in MDCK cells transiently expressing NKD2-EGFP and AKAP12-mCherry (Figure 5B).

**FIGURE 3** NKD2 S223 phosphorylation-deficient mutants reduce NKD2 stability and cell-surface delivery of TGF $\alpha$ . A, MDCK cells stably expressing NKD2-EGFP (upper panel) or (S223A)NKD2-EGFP (lower panel) were treated with cycloheximide (CHX, 20  $\mu$ g/mL) to block protein synthesis for the indicated times. Cell lysates were subjected to NKD2 and  $\alpha$ -tubulin immunoblotting. B, Results from three independent experiments in A were quantified and presented as relative intensity (RI) of NKD2 signal normalized to  $\alpha$ -tubulin signal. C, MDCK cells were transiently transfected with TGF $\alpha$  along with NKD2-EGFP or (S223A)NKD2-EGFP as indicated. These cells were pretreated with the PKA inhibitor H89 (30  $\mu$ M) and/or the MMP inhibitor BB-94 (5  $\mu$ M) for 1 hour followed by FSK (1  $\mu$ M, 5 minutes) as indicated at 37°C. Cells were then cooled and incubated with anti-TGF $\alpha$  antibody under nonpermeabilized conditions at 4°C for 1 hour. Cells were then paraformaldehyde-fixed and stained for p120. Fluorescence associated with TGF $\alpha$ , p120 and NKD2 is displayed in red, blue and green, respectively. Scale bars: 10  $\mu$ m

**FIGURE 4** EGFR transactivation is dependent on PKA/NKD2/MMP-mediated TGF $\alpha$  release. A, Conditioned media from overnight cultures (16–24 hours) of MDCK cells transiently transfected with indicated plasmid constructs were collected. One hour prior to collection of conditioned media, the cultures were incubated with the antibodies indicated. Conditioned media were then added to serum-starved A431 cells for 5 minutes. Recipient A431 cells were lysed and subjected to EGFR IP with subsequent immunoblotting for pY1173-EGFR and total EGFR. B, Caco-2 cells engineered to express TGF $\alpha$  under doxycycline control (Caco-2 iTGF $\alpha$ ) were incubated with the GPCR agonist VIP (100 nM) for the indicated times in the TGF $\alpha$ -induced or -uninduced state and then lysed. Lysates were subjected to EGFR IP followed by immunoblotting for phospho-tyrosine (pY) and EGFR. The image is representative of three independent experiments. C, Caco-2 iTGF $\alpha$  cells in the induced state were preincubated with H89 (30  $\mu$ M) or BB-94 (5  $\mu$ M) for 1 hour, stimulated with VIP (100 nM) and lysed after 1 minute as indicated. Lysates were subjected to EGFR IP followed by immunoblotting for pY and EGFR. Corresponding total lysates were immunoblotted for TGF $\alpha$  and  $\beta$ -actin to show equal expression and loading



To assess the functional consequence of the interaction between NKD2 and AKAP12, we deleted AKAP12 in HEK293 cells by clustered regularly interspaced short palindromic repeats/Cas9 (CRISPR/Cas9) gene editing; the decrease in AKAP12 was documented by AKAP12 immunoblots in the right two lanes in Figure 5C. Under baseline conditions, pS223-NKD2 was barely detectable in AKAP12 knockout cells and the signal was markedly reduced following FSK stimulation compared to parental HEK293 cells (quantified in Figure 5D).

## 2.5 | AKAP12 mediates phosphorylation of NKD2 in the cytoplasm

We then examined the ability of FSK and the G $\alpha$ s-associated GPCR agonists, VIP and PGE $_2$ , to induce phosphorylation of NKD2 in parental and AKAP12 knockout HEK293 cells. As expected, all three stimuli led to phosphorylation of NKD2 S223 within 30 seconds in parental HEK293 cells (Figure 6A, left panels). However, in AKAP12 knockout HEK293 cells, these stimuli failed to induce NKD2 S223 phosphorylation (Figure 6A, right panels). The merged images from the left panels

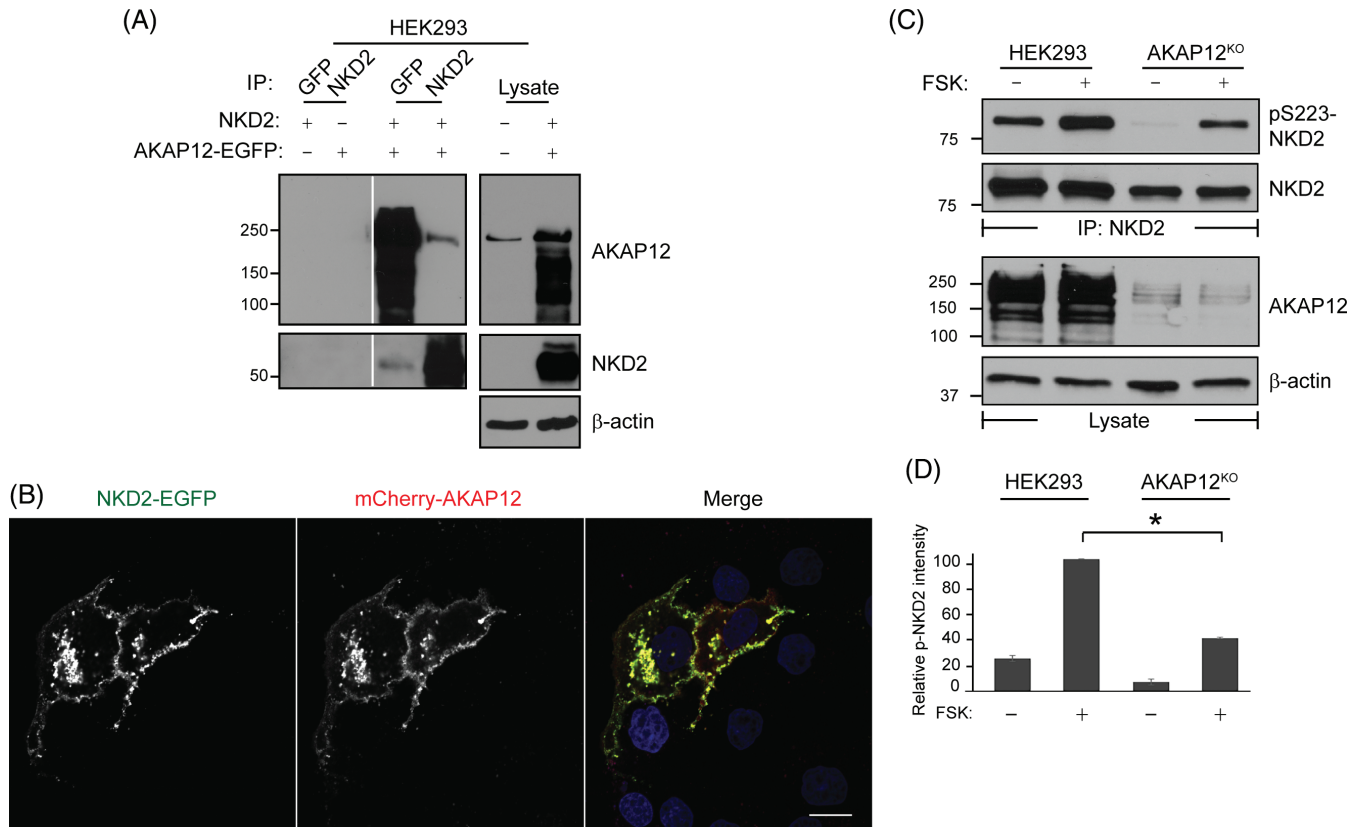


**FIGURE 5** AKAP12 and NKD2 interaction is necessary for NKD2 phosphorylation. A, Lysates from HEK293 cells transiently expressing NKD2 and AKAP12-EGFP were prepared and subjected to IP with GFP or NKD2 antibodies followed by immunoblotting with AKAP12 and NKD2 antibodies as indicated. Right panel shows whole-cell lysates immunoblotted for AKAP12, NKD2, and β-actin as input controls. B, MDCK cells transiently expressing NKD2-EGFP (green) and mCherry-AKAP12 (red) were fixed and stained with DAPI (blue). Scale bar: 10 μm. C, Parental and CRISPR/Cas9-based AKAP12 knockout (AKAP12<sup>KO</sup>) HEK293 cells were transiently transfected with NKD2-EGFP and incubated in the presence or absence of FSK (1 μM) for 5 minutes. Cells were then lysed and subjected to immunoblotting with the indicated antibodies. D, Quantification of (C) from three independent experiments; \* indicates  $P < 0.05$

show colocalization (white) of AKAP12 and NKD2 occurring mostly in cytoplasmic puncta. To confirm that AKAP12-mediated phosphorylation of NKD2 occurs in the cytoplasm, we tested whether FSK induced phosphorylation of the myristoylation-defective (G2A)NKD2 mutant. In Figure 6B, we show that FSK increased phosphorylation of (G2A)NKD2 that is restricted to the cytoplasm.

AKAP12 is a dual-specificity AKAP that interacts with both PKA regulatory subunit I (RI) and PKA regulatory subunit II (RII) isoforms of PKA.<sup>33</sup> To determine if this transactivation phenomenon is dependent on RI or RII, we used two stapled peptides, the RI-selective Stapled AKAP Disruptor 2 (RI-STAD-2), and the RII-selective STAD-2.<sup>34,35</sup> Both of these peptides attenuated FSK-induced NKD2 phosphorylation, indicating both PKA isoforms can phosphorylate NKD2 at S223 (Figure 6C). However, the RII-selective STAD-2 had a greater inhibitory effect than RI-specific RI-STAD-2, suggesting a preference for RII in mediating NKD2 phosphorylation (quantified in Figure S4).

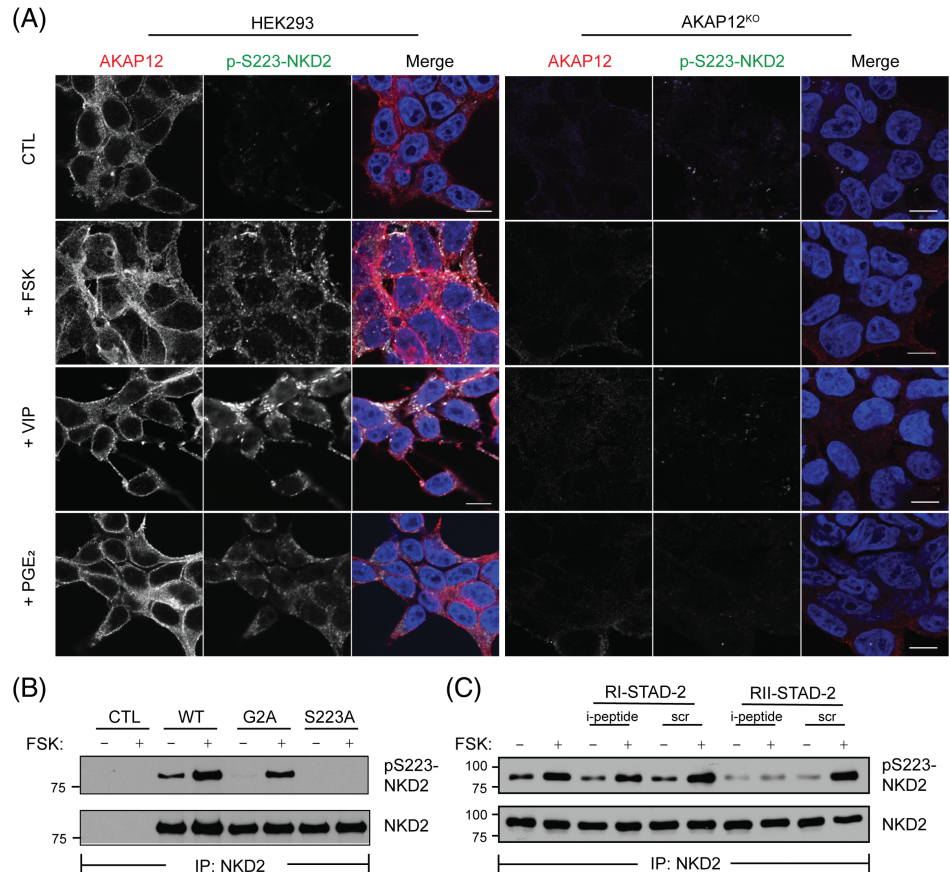
Thus, AKAP12 is required for GPCR-induced PKA-mediated NKD2 S223 phosphorylation and subsequent TGFα release and EGFR activation.

### 3 | DISCUSSION

These studies identify a new mode of GPCR-mediated EGFR transactivation. In classical EGFR transactivation, activation of GPCRs induces MMP-mediated cleavage of membrane-anchored EGFR ligands to release soluble ligands that then bind and activate EGFRs. We now show that the GPCR ligands VIP and PGE<sub>2</sub> transactivate EGFR by increasing cell-surface delivery of TGFα, a step that precedes ligand cleavage (Figure 4). Mechanistically, VIP and PGE<sub>2</sub> activate PKA that then phosphorylates NKD2 S223 (Figures 1 and 2). This phosphorylation stabilizes NKD2, a selective basolateral sorting adaptor for TGFα; this stabilization of NKD2 enhances delivery of TGFα to the cell surface and results in increased EGFR activation (Figures 3 and 4).

These results are shown using different epithelial cell lines (HEK293 and polarizing MDCK, Caco-2 and HCA-7). When possible, we chose lines in which we could examine endogenous elements. For example, we examined the effects of VIP on phosphorylation of endogenous NKD2 in polarized Caco-2 and HCA-7 cells. We actually took advantage of the fact that Caco-2 cells do not express TGFα. By inducibly overexpressing TGFα in these cells, we were able to show

**FIGURE 6** AKAP12 and NKD2 interact intracellularly during GPCR-induced NKD2 phosphorylation. A, Parental and AKAP12<sup>KO</sup> HEK293 cells were incubated with FSK, VIP or PGE<sub>2</sub> for 30 seconds as indicated and were then fixed and stained for AKAP12 (red) and pS223-NKD2 (green). Scale bars: 10  $\mu$ m. B, FSK was added to HEK293 cells transiently expressing either wild-type, (G2A)NKD2 or (S223A)NKD2. Lysates were immunoprecipitated with NKD2 or IgG control antibodies followed by immunoblotting for pS223-NKD2 and NKD2. C, HEK293 cells transiently expressing NKD2-EGFP were incubated with stapled inhibitory peptides (i-peptide) RI-STAD-2 (RI-selective) and STAD-2 (RII-selective) or their corresponding scrambled (scr) peptides (5  $\mu$ M) for 1 hour and stimulated with FSK (0.5  $\mu$ M) for 5 minutes. Cells were then lysed and subjected to IP with NKD2 antibodies followed by immunoblotting for pS223-NKD2 and NKD2



that EGFR transactivation is dependent on TGF $\alpha$  via endogenous PKA/NKD2/MMP-mediated events (Figure 4B).

As noted in the introduction, NKD2 is a short-lived protein that is polyubiquitylated in the cytoplasm by the E3 ligase RNF25.<sup>17</sup> It is stabilized by interacting with TGF $\alpha$  in exocytic vesicles that are directed to the basolateral surface of polarized epithelial cells where the vesicles dock and fuse in a NKD2 myristoylation-dependent manner.<sup>15–17</sup> These effects of NKD2 appear to be selective for TGF $\alpha$  because delivery of two other basolaterally targeted EGFR ligands, amphiregulin and epiregulin, is not impaired in myristoylation-deficient (G2A) NKD2-expressing cells.<sup>36,37</sup>

The present studies were initially designed to determine whether NKD2 was phosphorylated in addition to previously reported ubiquitylation and myristoylation. We show that NKD2 phosphorylation was induced by the PKA agonist FSK but not by the PKC agonist TPA (Figure 1B and Table S1). Moreover, PKA activation selectively phosphorylates NKD2 at S223 (Figure 1D), resulting in stabilization of NKD2 (Figure 3A,B). The half-life of the (S223A)NKD2 mutant is half as long as wild-type NKD2, resulting in less efficient delivery of its cargo TGF $\alpha$  and decreased EGFR activation (Figures 3 and 4). We also performed experiments with physiological stimuli like the GPCR ligands VIP, PGE<sub>2</sub> and carbachol. VIP and PGE<sub>2</sub> selectively induced NKD2 S223 phosphorylation and subsequent EGFR activation, which could be blocked by the PKA inhibitor H89 (Figure 1F). These results show that in addition to inducing cleavage of EGFR ligands, GPCR ligands can enhance NKD2-mediated delivery of TGF $\alpha$  to the cell surface. This new mode of regulation preferentially employs G $\alpha$ s-associated GPCRs.

It is well established that the localized effects of PKA within the cell are achieved by PKA binding to different AKAPs. As noted above, AKAP12 (alias Gravin or AKAP250) was the only AKAP found in a comprehensive proteomic analysis of NKD2-associated vesicles.<sup>29</sup> AKAP12 is found in multiple cellular compartments, including the plasma membrane, cytosol, and nucleus, and it has been assigned specific roles in each of these compartments.<sup>38</sup> AKAP12 has been touted to be a tumor suppressor, and even more specifically, a metastasis suppressor; Gelman and coworkers identified AKAP12 as a gene downregulated by v-Src and named Src-Suppressed C Kinase Substrate (SScCKS) and given the moniker “essex.”<sup>32,39</sup> A number of functional domains have been identified in AKAP12, including a second residue glycine that is myristoylated.<sup>40</sup> AKAP12 associates with both PKA and PKC. Grove and coworkers reported that activation of PKC redistributes AKAP12 from the plasma membrane to punctate perinuclear vesicles, leading these investigators to speculate that it represents an example of PKC and PKA crosstalk.<sup>41</sup> Under our experimental conditions, TPA activation of PKC did not result in phosphorylation of NKD2, but FSK activation of PKA resulted in phosphorylation of S223 NKD2 (Figure 1B). Importantly, we showed AKAP12 interacts with NKD2 and that this interaction occurs within specific subcellular locations in the cell (Figures 5A,B and 6A,B). Finally, AKAP12 knockout abrogated baseline phosphorylation of S223 NKD2 and attenuated S223 NKD2 phosphorylation induced in response to FSK, VIP and PGE<sub>2</sub> (Figure 6A).

Because GPCR transactivation of EGFR was discovered over 20 years ago, it has become a well-accepted, clinically relevant biological phenomenon that has been extended to multiple diverse stimuli

that indirectly activate EGFR and other RTKs.<sup>3,42,43</sup> Most often this is because of activation of MMPs, which release cell-surface anchored ligands, although ligand-independent transactivation also occurs.<sup>44</sup> The present studies have uncovered an additional step in ligand-dependent transactivation, that is, GPCR-triggered cell-surface delivery of TGF $\alpha$ . Thus, both EGFR ligand delivery and cleavage may be regulated by GPCR agonists to enhance EGFR activity. Future work will be needed to determine if different GPCR ligands exhibit a preference for acting at one or both of these steps. This transactivation mechanism is currently limited to the EGFR ligand TGF $\alpha$  because, as noted above, NKD2 is a selective adaptor for TGF $\alpha$ .<sup>36,37</sup> Going forward, it will be of interest to determine if trafficking adaptors for other RTK ligands are regulated in a similar fashion. In the broader context, our work highlights a convergence point between GPCR and RTK signaling where GPCR activation facilitates intracellular trafficking of a RTK ligand, leading to increased RTK activity.

## 4 | MATERIALS AND METHODS

### 4.1 | Plasmids, antibodies and other reagents

The construction and expression of human NKD2 (NP\_149111.1) fused with EGFP has been previously described.<sup>15</sup> All NKD2 site mutants were generated either by Stratagene's quick change site-directed mutagenesis kit or by polymerase chain reaction (PCR) overlap extension. Human AKAP12-HA was kindly provided by Craig C. Malbon (State University of New York at Stony Brook). All chemicals, including paraformaldehyde,  $\beta$ -actin antibody, doxycycline, FSK, H89, and protease inhibitor cocktails, were from Sigma unless otherwise stated. Chemicals for electrophoresis and protein markers were purchased from Bio-Rad. Anti-human NKD2 antibody (R44) and TGF $\alpha$  polyclonal antibody were generated by Covance.<sup>15</sup> Mouse NKD2 antibody was a kind gift from Tianhui Hu and Jianhua Yan's Lab.<sup>45</sup> AKAP12 antibody (cat#: PA5-21759, RRID:AB\_11154150), Protein G beads and Mammalian Protein Extraction Reagent (M-PER) were purchased from ThermoFisher Scientific and mouse AKAP12 antibody from Abcam (ab49849, RRID:AB\_2225608). E-cadherin and  $\alpha$ -tubulin antibodies along with cycloheximide, were purchased from EMD Millipore. pS223-NKD2 antibody was raised in rabbits (EZBiolab Inc.) against NKD2 peptide (HVRRPpSTDPQPC) and affinity purified with the same peptide.

### 4.2 | Cell culture, generation of MDCK cells stably expressing NKD2-EGFP or (S223A)NKD2-EGFP and Caco-2 iTGF $\alpha$ cells

All cell culture media and supplements were purchased from HyClone. HEK293, Caco-2 and MDCK cells were maintained in DMEM supplemented with 10% fetal bovine serum (FBS), L-glutamine, non-essential amino acids, 100 units/mL penicillin, 100  $\mu$ g/mL streptomycin at 37°C with 5% CO<sub>2</sub>. To generate NKD2 and its serine/threonine mutant-expressing stable cell lines, the Retro-X Tet-Off Advanced Inducible Expression System was used (Clontech), according to the manufacturer's instructions. HEK293 cells packaged with a viral

envelope expression vector (Retro-X System) were transiently transfected with pRetroX-tight-pur-NKD2-EGFP or its mutants for 24 hours using Metafectene transfection reagent (Biontech Laboratories GmbH). Virus-containing medium (supernatant) from packaging cells was collected and filtered through a 0.45  $\mu$ m filter. After removing cells and debris, supernatant was added to cultured MDCK II Tet-off T23 1628 cells (Clontech) or Caco-2 cells. Twenty-four hours after infection, cells were selected in the presence of 500  $\mu$ g/mL Geneticin, 5  $\mu$ g/mL puromycin (EMD Millipore) and 0.5  $\mu$ g/mL doxycycline. Positive pools were subsequently cloned by limiting dilution. To test protein expression, cells were completely washed with cold 1 $\times$  PBS three times and then maintained in DMEM with 10% FBS for at least 24 hours. For polarization experiments with MDCK cells, 1  $\times$  10<sup>5</sup> cells were seeded on 12-mm Transwell filters (0.4  $\mu$ m; Corning Costar) and cultured for 4-5 days with replenishment of medium every other day until trans-epithelial electrical resistance exceeded 200  $\Omega$ /cm<sup>2</sup> measured using the Millicell Electrical Resistance System (EMD Millipore).

### 4.3 | Phosphorylation of NKD2 in vitro

NKD2-EGFP-expressing MDCK cells were induced by growth in tet-off medium for 24 hours in 100 mm Petri dishes (1.5  $\times$  10<sup>7</sup> cells/plate). The plates were washed three times with precooled tris buffered saline (TBS) and incubated for 60 minutes at 37°C in phosphate-free medium (Sol. D: 50 mM HEPES, 78 mM KCl, 4 mM MgCl<sub>2</sub>, 8 mM CaCl<sub>2</sub> and 10 mM EGTA, pH 7.0). The medium was removed and 138  $\mu$ Ci <sup>32</sup>P orthophosphate in DMEM (without phosphate) was added for 2 hours. Cells were washed with precooled TBS buffer with phosphatase inhibitors, then lysed in 0.75 mL M-PER with 1 $\times$  phosphatase inhibitor cocktail (PhosStop), 10  $\mu$ M phenylarsineoxide, tyrosine phosphatase inhibitor (Sigma), 1 mM sodium ortho vanadate (Sigma) and 10 mM sodium fluoride. The supernatant was incubated with NKD2 antibody precoupled to protein G-conjugated agarose beads overnight at 4°C. NKD2 IPs were then washed and analyzed by immunoblotting and autoradiography.

### 4.4 | Immunoprecipitation and immunoblotting

HEK293 cells were transfected with 0.1  $\mu$ g of plasmid DNA (NKD2, NKD2-EGFP and/or AKAP12-EGFP) using polyethylenimine (PEI) as indicated. Twenty-four hours after transfection, cells were washed twice with PBS and lysed in 1-4 times diluted M-PER lysis buffer containing 1 $\times$  PhosStop and 1 $\times$  protease inhibitor cocktails. Cell lysates were centrifuged at 14 000 rpm for 5 minutes, and the supernatants were mixed with protein G beads and incubated with NKD2, green fluorescent protein (GFP) or AKAP12 antibodies at 4°C overnight. The beads were washed six times with radioimmunoprecipitation assay buffer, and bound proteins were eluted by boiling in urea sample buffer (8 M urea, 0.125 M Tris-HCl, 2% SDS, 10%  $\beta$ -mecapthanol-15% glycerol, pH 6.8) or M-PER lysis buffer. Laemmli loading dye was added to eluates, which were then resolved on SDS-PAGE and subjected to immunoblotting with the indicated antibodies.

#### 4.5 | CRISPR/Cas9-based knockout of endogenous AKAP12 in HEK293 parental cells

A pair of AKAP12 CRISPR/Cas9 knockout plasmids were each encoding a D10A mutated Cas9 nuclease and a unique, target-specific 20 nucleotide guide RNA (gRNA): 5'-ctccaggagggtgacctaaa and opposite 5'-ctcagctacgccattgatgg (sc-406008; Santa Cruz Biotechnology, Inc.). One plasmid in the pair contained a puromycin resistance gene for selection; the other plasmid in the pair contained a GFP marker to visually confirm transfection. GFP expression was monitored 48 hours post-transfection, and after 72 hours cells were switched into puromycin media (0.3 µg/mL) for selection of cells where successful Cas9-induced double strand breaks had occurred. The cells were resuspended in cold OptiMEM, passed through a 40 µm pore size cell strainer, cloned by limiting dilution and screened for GFP fluorescence.

#### 4.6 | Immunofluorescence and confocal microscopy

Cells were grown on plastic or on 12-mm Transwell filters typically for 2 or 5 days, respectively. Cells were then washed with PBS and fixed with 4% paraformaldehyde (PFA) for 10 minutes at room temperature (RT), permeabilized with 0.5% Triton X-100 for 5 minutes (RT) and then blocked for 1 hour in 5% BSA at 4°C. All incubations were performed in PBS. For TGF $\alpha$  cell-surface labeling, cells were first incubated with TGF $\alpha$  antibody at 4°C in PBS for 1 hour, washed 3 $\times$  with PBS to remove excess unbound antibody and then fixed and processed for immunofluorescence as described above. Microscopy was performed with Zeiss LSM 710 or Nikon A1R confocal microscopes.

#### 4.7 | Statistics

Statistical analyses were performed using GraphPad Prism software (version 7.02; GraphPad Software, Inc.). All measurements were normalized to the highest value and plotted as mean  $\pm$  SD. Significance determination was performed by ordinary one-way analysis of variance followed by Tukey's multiple comparisons test, with a single pooled variance;  $P < 0.05$  was considered statistically significant between the pairs tested.

#### ACKNOWLEDGMENTS

The authors thank Graham Carpenter for advice and encouragement throughout the course of these studies, Yu-Ping Yang for model illustration and Hai Cui for statistical analysis. The studies were supported by R01 DK48370 and R01 DK70856 to J.R.G., R35 CA197570 and P50 CA095103 to R.J.C., R03 CA188439 to E.J.K., Vanderbilt Digestive Diseases Research Center P30 DK058404 and Vanderbilt-Ingram Cancer Center P30 CA068485.

#### CONFLICT OF INTEREST

The authors declare that they have no conflicts of interest with the contents of this article.

The content is solely the responsibility of the authors and does not necessarily represent the official views of the National Institutes of Health.

#### AUTHOR CONTRIBUTIONS

Z.C., B.S., C.L. and R.J.C. designed research. Z.C., B.S., C.L., L.J.C., J.L.F. and R.G.D. performed research; Z.C., B.S., C.L., N.O.M., J.L.F., J.R.G., E.J.K., J.R.G. and R.J.C. analyzed the data and provided critical input and B.S., Z.C., N.O.M. and R.J.C. wrote the manuscript.

#### ORCID

Bhuminder Singh  <https://orcid.org/0000-0003-1357-2158>

Nicholas O. Markham  <https://orcid.org/0000-0002-1348-1267>

Léolène J. Carrington  <https://orcid.org/0000-0002-7352-3270>

Jeffrey L. Franklin  <https://orcid.org/0000-0002-7111-4449>

Eileen J. Kennedy  <https://orcid.org/0000-0001-5610-1677>

James R. Goldenring  <https://orcid.org/0000-0002-7833-2940>

Robert J. Coffey  <https://orcid.org/0000-0002-2180-3844>

#### REFERENCES

- Katritch V, Cherezov V, Stevens RC. Structure-function of the G protein-coupled receptor superfamily. *Annu Rev Pharmacol Toxicol.* 2013;53:531-556.
- Lemmon MA, Schlessinger J. Cell signaling by receptor tyrosine kinases. *Cell.* 2010;141(7):1117-1134.
- Kose M. GPCRs and EGFR—cross-talk of membrane receptors in cancer. *Bioorg Med Chem Lett.* 2017;27(16):3611-3620.
- Forrester SJ, Kawai T, O'Brien S, Thomas W, Harris RC, Eguchi S. Epidermal growth factor receptor transactivation: mechanisms, pathophysiology, and potential therapies in the cardiovascular system. *Annu Rev Pharmacol Toxicol.* 2016;56:627-653.
- Daub H, Weiss FU, Wallasch C, Ullrich A. Role of transactivation of the EGF receptor in signalling by G-protein-coupled receptors. *Nature.* 1996;379(6565):557-560.
- Prenzel N, Zwick E, Daub H, et al. EGF receptor transactivation by G-protein-coupled receptors requires metalloproteinase cleavage of proHB-EGF. *Nature.* 1999;402(6764):884-888.
- Wang T, Li Z, Cvijic ME, Zhang L, Sum CS. Measurement of cAMP for Galphas- and Galphai Protein-Coupled Receptors (GPCRs). In: Sittampalam GS, Coussens NP, Brimacombe K, et al., eds. *Assay Guidance Manual.* Bethesda, MD: Eli Lilly & Company and the National Center for Advancing Translational Sciences; 2004:797-822.
- Bertelsen LS, Barrett KE, Keely SJ. Gs protein-coupled receptor agonists induce transactivation of the epidermal growth factor receptor in T84 cells: implications for epithelial secretory responses. *J Biol Chem.* 2004;279(8):6271-6279.
- Scott JD, Dessauer CW, Tasken K. Creating order from chaos: cellular regulation by kinase anchoring. *Annu Rev Pharmacol Toxicol.* 2013;53:187-210.
- Chen N, Ma W-Y, She Q-B, et al. Transactivation of the epidermal growth factor receptor is involved in 12-O-tetradecanoylphorbol-13-acetate-induced signal transduction. *J Biol Chem.* 2001;276(50):46722-46728.
- Singh B, Carpenter G, Coffey RJ. EGF receptor ligands: recent advances. *F1000Res.* 2016;5:1-11.

12. Singh B, Coffey RJ. From wavy hair to naked proteins: the role of transforming growth factor alpha in health and disease. *Semin Cell Dev Biol.* 2014;28:12-21.
13. Singh B, Coffey RJ. Trafficking of epidermal growth factor receptor ligands in polarized epithelial cells. *Annu Rev Physiol.* 2014;76:275-300.
14. Dempsey PJ, Coffey RJ. Basolateral targeting and efficient consumption of transforming growth factor- $\alpha$  when expressed in Madin-Darby canine kidney cells. *J Biol Chem.* 1994;269(24):16878-16889.
15. Li C, Franklin JL, Graves-Deal R, Jerome WG, Cao Z, Coffey RJ. Myristoylated Naked2 escorts transforming growth factor alpha to the basolateral plasma membrane of polarized epithelial cells. *Proc Natl Acad Sci U S A.* 2004;101(15):5571-5576.
16. Li C, Hao M, Cao Z, et al. Naked2 acts as a cargo recognition and targeting protein to ensure proper delivery and fusion of TGF- $\alpha$  containing exocytic vesicles at the lower lateral membrane of polarized MDCK cells. *Mol Biol Cell.* 2007;18(8):3081-3093.
17. Ding W, Li C, Hu T, et al. EGF receptor-independent action of TGF- $\alpha$  protects Naked2 from AO7-mediated ubiquitylation and proteasomal degradation. *Proc Natl Acad Sci U S A.* 2008;105(36):13433-13438.
18. Blom N, Gammeltoft S, Brunak S. Sequence and structure-based prediction of eukaryotic protein phosphorylation sites. *J Mol Biol.* 1999;294(5):1351-1362.
19. Pearson D, Nigg EA, Nagamine Y, Jans DA, Hemmings BA. Mechanisms of cAMP-mediated gene induction: examination of renal epithelial cell mutants affected in the catalytic subunit of the cAMP-dependent protein kinase. *Exp Cell Res.* 1991;192(1):315-318.
20. Montminy M. Transcriptional regulation by cyclic AMP. *Annu Rev Biochem.* 1997;66:807-822.
21. Nishikawa K, Tokar A, Johannes FJ, Songyang Z, Cantley LC. Determination of the specific substrate sequence motifs of protein kinase C isozymes. *J Biol Chem.* 1997;272(2):952-960.
22. Buchanan FG, Wang D, Bargiacchi F, DuBois RN. Prostaglandin E2 regulates cell migration via the intracellular activation of the epidermal growth factor receptor. *J Biol Chem.* 2003;278(37):35451-35457.
23. Keely SJ, Calandrella SO, Barrett KE. Carbachol-stimulated transactivation of epidermal growth factor receptor and mitogen-activated protein kinase in T(84) cells is mediated by intracellular Ca<sup>2+</sup>, PYK-2, and p60(src). *J Biol Chem.* 2000;275(17):12619-12625.
24. Fogh J, Fogh JM, Orfeo T. One hundred and twenty-seven cultured human tumor cell lines producing tumors in nude mice. *J Natl Cancer Inst.* 1977;59(1):221-226.
25. Kirkland SC. Dome formation by a human colonic adenocarcinoma cell line (HCA-7). *Cancer Res.* 1985;45(8):3790-3795.
26. Hunter T, Cooper JA. Epidermal growth factor induces rapid tyrosine phosphorylation of proteins in A431 human tumor cells. *Cell.* 1981;24(3):741-752.
27. Calejo AI, Tasken K. Targeting protein-protein interactions in complexes organized by A kinase anchoring proteins. *Front Pharmacol.* 2015;6:192.
28. Seino S, Shibasaki T. PKA-dependent and PKA-independent pathways for cAMP-regulated exocytosis. *Physiol Rev.* 2005;85(4):1303-1342.
29. Cao Z, Li C, Higginbotham JN, et al. Use of fluorescence-activated vesicle sorting for isolation of Naked2-associated, basolaterally targeted exocytic vesicles for proteomics analysis. *Mol Cell Proteomics.* 2008;7(9):1651-1667.
30. Schott MB, Gonowolo F, Maliske B, Grove B. FRET biosensors reveal AKAP-mediated shaping of subcellular PKA activity and a novel mode of Ca(2+)/PKA crosstalk. *Cell Signal.* 2016;28(4):294-306.
31. Willoughby D, Wong W, Schaack J, Scott JD, Cooper DM. An anchored PKA and PDE4 complex regulates subplasmalemmal cAMP dynamics. *EMBO J.* 2006;25(10):2051-2061.
32. Gelman IH. Emerging roles for SSeCKS/Gravin/AKAP12 in the control of cell proliferation, cancer malignancy, and barrierogenesis. *Genes Cancer.* 2010;1(11):1147-1156.
33. Aye TT, Mohammed S, van den Toorn HW, et al. Selectivity in enrichment of cAMP-dependent protein kinase regulatory subunits type I and type II and their interactors using modified cAMP affinity resins. *Mol Cell Proteomics.* 2009;8(5):1016-1028.
34. Wang Y, Ho TG, Bertinetti D, et al. Isoform-selective disruption of AKAP-localized PKA using hydrocarbon stapled peptides. *ACS Chem Biol.* 2014;9(3):635-642.
35. Wang Y, Ho TG, Franz E, et al. PKA-type I selective constrained peptide disruptors of AKAP complexes. *ACS Chem Biol.* 2015;10(6):1502-1510.
36. Gephart JD, Singh B, Higginbotham JN, et al. Identification of a novel mono-leucine basolateral sorting motif within the cytoplasmic domain of amphiregulin. *Traffic.* 2011;12(12):1793-1804.
37. Singh B, Bogatcheva G, Washington MK, Coffey RJ. Transformation of polarized epithelial cells by apical mistrafficking of ephregulin. *Proc Natl Acad Sci U S A.* 2013;110(22):8960-8965.
38. Rababa'h A, Singh S, Suryavanshi SV, Altarabsheh SE, Deo SV, McConnell BK. Compartmentalization role of A-kinase anchoring proteins (AKAPs) in mediating protein kinase A (PKA) signaling and cardiomyocyte hypertrophy. *Int J Mol Sci.* 2014;16(1):218-229.
39. Gelman IH. Suppression of tumor and metastasis progression through the scaffolding functions of SSeCKS/Gravin/AKAP12. *Cancer Metastasis Rev.* 2012;31(3-4):493-500.
40. Malbon CC, Tao J, Shumay E, Wang HY. AKAP (A-kinase anchoring protein) domains: beads of structure-function on the necklace of G-protein signalling. *Biochem Soc Trans.* 2004;32(Pt 5):861-864.
41. Yan X, Walkiewicz M, Carlson J, Leiphon L, Grove B. Gravin dynamics regulates the subcellular distribution of PKA. *Exp Cell Res.* 2009;315(7):1247-1259.
42. Wang Z. Transactivation of epidermal growth factor receptor by G protein-coupled receptors: recent Progress, challenges and future research. *Int J Mol Sci.* 2016;17(1):1-12.
43. Singh B, Schneider M, Knyazev P, Ullrich A. UV-induced EGFR signal transactivation is dependent on prolignand shedding by activated metalloproteases in skin cancer cell lines. *Int J Cancer.* 2009;124(3):531-539.
44. Drube S, Stirnweiss J, Valkova C, Liebmann C. Ligand-independent and EGF receptor-supported transactivation: lessons from beta2-adrenergic receptor signalling. *Cell Signal.* 2006;18(10):1633-1646.
45. Cao C, Wang S, Lv S, et al. A monoclonal antibody produced against Naked2. *Monoclon Antib Immunodiagn Immunother.* 2013;32(4):290-294.

## SUPPORTING INFORMATION

Additional supporting information may be found online in the Supporting Information section at the end of this article.

**How to cite this article:** Cao Z, Singh B, Li C, et al. Protein kinase A-mediated phosphorylation of naked cuticle homolog 2 stimulates cell-surface delivery of transforming growth factor- $\alpha$  for epidermal growth factor receptor transactivation. *Traffic.* 2019;20:357-368. <https://doi.org/10.1111/tra.12642>